Check for updates

The microRNA-30 family targets *DLL4* to modulate endothelial cell behavior during angiogenesis

Gemma Bridge,[1] Rui Monteiro,[2] Stephen Henderson,[1] Victoria Emuss,[1] Dimitris Lagos,[3] Dimitra Georgopoulou,[1] Roger Patient,[2] and Chris Boshoff[1]

[1]Cancer Research UK Viral Oncology Group, UCL Cancer Institute, University College London, London, United Kingdom; [2]MRC Molecular Haematology Unit, The Weatherall Institute of Molecular Medicine, University of Oxford, Oxford, United Kingdom; and [3]Centre for Immunology and Infection, Department of Biology and Hull York Medical School, University of York, York, United Kingdom

Delta-like 4 (DLL4), a membrane-bound ligand belonging to the Notch signaling family, plays a fundamental role in vascular development and angiogenesis. We identified a conserved microRNA family, miR-30, which targets *DLL4*. Overexpression of miR-30b in endothelial cells led to increased vessel number and length in an in vitro model of sprouting angiogenesis. Microinjection of miR-30 mimics into zebrafish embryos resulted in suppression of *dll4* and subsequent excessive sprouting of intersegmental vessels and reduction in dorsal aorta diameter. Use of a target protector against the miR-30 site within the *dll4* 3′UTR up-regulated *dll4* and synergized with Vegfa signaling knockdown to inhibit angiogenesis. Furthermore, restoration of miR-30b or miR-30c expression during Kaposi sarcoma herpesvirus (KSHV) infection attenuated viral induction of DLL4. Together these results demonstrate that the highly conserved molecular targeting of *DLL4* by the miR-30 family regulates angiogenesis. (*Blood*. 2012;120(25):5063-5072)

Introduction

DLL4 plays a fundamental role in vascular development and angiogenesis.[1,2] *DLL4* haploinsufficiency results in extensive arterial defects and embryonic lethality,[3] indicating that the developing vasculature is sensitive to minor alterations in DLL4 dosage. DLL4 expression is mainly restricted to the endothelium of nascent vessels, particularly the tip cells, where it maintains stalk cell identity in neighboring cells, thereby regulating vessel sprouting and branching in response to angiogenic stimuli.[4] The importance of optimal DLL4 expression in physiologic angiogenesis is illustrated through its regulation of intersegmental vessel (ISV) development in zebrafish. Morpholino (MO) knockdown of *dll4* in zebrafish results in an increased number of endothelial cells within the ISVs and ectopic ISV branching from the dorsal aorta (DA) because of overactivation of Vegfa signaling.[5,6]

DLL4 is relevant in pathologic angiogenesis and is overexpressed in human tumors, often in association with markers of inflammation, hypoxia and angiogenesis.[7-9] Inhibition of DLL4 suppresses experimental tumor growth by inducing nonproductive, deregulated angiogenesis.[10,11] We and others have shown that DLL4 expression is up-regulated in lymphatic endothelial cells (LECs) after infection by Kaposi sarcoma herpesvirus (KSHV),[12,13] an oncogenic γ-herpesvirus that is the etiologic agent of Kaposi sarcoma (KS). KS is an angioproliferative neoplasm composed of cells of endothelial origin.[14] Although accurate regulation of DLL4 levels is a hallmark of angiogenesis, the mechanisms that finely regulate DLL4 expression are not completely defined. Therefore we hypothesized that, in addition to well-known transcriptional mechanisms that affect *DLL4* expression, *DLL4* is regulated at the posttranscriptional level.

MicroRNAs (miRNAs) are small, noncoding RNAs that influence target gene expression through mRNA degradation and translation inhibition.[15] Implicated in key cellular processes, miRNAs play a role in angiogenesis and cancer.[16,17] miR-27b is the only miRNA thus far implicated in *DLL4* regulation[18]; however, this miRNA also regulates sprouty homologue 2 (*SPRY2*) and semaphorin 6A (*SEMA6A*), and it is unclear whether its proposed suppression of DLL4 specifically leads to vascular defects.[18,19] We previously described the miRNA signature in KSHV-infected LECs (KLECs).[20] These data indicated significant down-regulation of members of the miR-30 miRNA family postinfection (PI). Encoded by 6 genes and expressed from 4 distinct transcripts across the human genome, the members of the miR-30 family share an identical seed sequence and hence have common predicted targets.[21] Here we show that miR-30b and miR-30c target *DLL4* in vitro and in vivo, and that the miR-30 family regulates angiogenesis.

Methods

Cell culture

LECs were purchased from Promocell and grown in endothelial growth medium MV (Promocell) supplemented with 10 ng/mL VEGF-C (R&D Systems). HUVECs were purchased from Promocell and grown in endothelial growth medium MV2 (Promocell). For both LECs and HUVECs, experiments were performed before passage 8. BCBL-1 cells, latently infected with recombinant GFP-KSHV,[22] were cultured as previously described.[23] 293T and immortalized human fibroblast cells were grown in DMEM (Invitrogen), supplemented with 10% FBS.

Submitted April 16, 2012; accepted September 26, 2012. Prepublished online as *Blood* First Edition paper, October 18, 2012; DOI 10.1182/blood-2012-04-423004.

The online version of this article contains a data supplement.

The publication costs of this article were defrayed in part by page charge payment. Therefore, and solely to indicate this fact, this article is hereby marked "advertisement" in accordance with 18 USC section 1734.

© 2012 by The American Society of Hematology

Downloaded from http://ashpublications.org/blood/article-pdf/120/25/5063/1359076/zh805112005063.pdf by guest on 19 May 2024

KSHV production and infection of LECs

KSHV was produced and used to infect LECs as previously described.[23] This procedure reproducibly resulted in 30% to 50% of LECs expressing GFP 3 days after infection.

MicroRNA mimics and inhibitors

LECs and HUVECs were seeded in 6-well plates at 5×10^4 cells per well and 293T were seeded in 12-well plates at 2.5×10^4 cells per well, 16 hours before transfection. miRIDIAN miRNA mimics and inhibitors for hsa-miR-30b, hsa-miR-30c, and the negative control No. 1 (nontargeting control; Thermo Scientific) were transfected at 100nM, unless otherwise stated. Cells were harvested for RNA or protein, used for the hanging drop assay, or transfected with luciferase reporter plasmids 48 hours after transfection.

Western blotting

LECs or HUVECs were lysed in Pierce M-PER buffer (ThermoScientific). Equal amounts of protein were resolved on a 10% polyacrylamide gel. Antibodies against DLL4 (Cell Signaling Technology), GAPDH (Monoclonal 6C5, Advanced ImmunoChemical) and α-tubulin (Monoclonal B-5-1-2, Sigma-Aldrich) were detected with HRP-conjugated secondary antibodies and were quantified using ECL or ECL Plus (GE Healthcare).

Lentivirus production and infection of LECs and HUVECs

Genomic fragments containing pre–miR-30b and pre–miR-30c-1 were cloned from LECs and were expressed using a modified pSIN-MCS lentiviral vector as described,[23] subsequently referred to as pSIN_30b and pSIN_30c, respectively. The number of lentiviral copies per cell was determined by qPCR and miRNA expression was confirmed by qRT-PCR. Cells were infected in suspension. Experiments were performed 2 to 3 days after infection.

Quantitative PCR and quantitative RT-PCR

Genomic DNA for qPCR was extracted using the QIAamp DNA mini-kit (QIAGEN). The number of lentiviral copies per cell (c/c) was determined as previously described.[23] Total RNA was extracted using the miRNeasy mini-kit (QIAGEN) and subjected to DNase I treatment (QIAGEN). For zebrafish work, RNA was collected from at least 10 embryos per condition or time point. Approximately 50 to 1000 ng of total RNA were used for cDNA synthesis using the SuperScript II reverse transcriptase (Invitrogen). *GAPDH* (housekeeping reference gene) and *SELE* mRNA levels were quantified by qRT-PCR using optimized forward and reverse primers at 0.3μM and SYBR Green PCR master mix (Applied Biosystems). The *GAPDH* primers used were as follows: forward primer 5′-GGAGTCAACGGATTTGGTCGTA-3′; reverse primer 5′-GGCAACAATATCCACTTTACCAGAGT-3′. The *SELE* primers used were as follows: forward primer 5′-CAGCCTCAAGATCATCAGCA-3′; reverse primer 5′-ACAGTCTTCTGGGTGGCAGT-3′. qRT-PCR quantification of *DLL4*, *dll4*, *bactin1*, miR-30b, and miR-30c was performed using Taqman gene expression or Taqman microRNA assays (Applied Biosystems). Quantification of pre–miR-30c-1 and pre–miR-30c-2 was performed using miRNA qRT-PCR Kit and Primer Set (GenoExplorer).

Luciferase reporter assay

The reporter plasmids (50 ng), either empty vector (pEZX-MT01) or the *DLL4* 3′UTR containing plasmid (pEZX-*DLL4*), were transfected into 293T cells, 48 hours after transfection with miRNA mimic. Cells were harvested 24 hours after transfection according to the Dual-Luciferase Reporter assay system (Promega). Luciferase activity was measured using a Fluoroskan Ascent FL luminometer (ThermoScientific). Firefly activity was normalized to internal renilla luciferase levels.

3-D spheroid in vitro angiogenesis assay

HUVECs were transfected with miRNA mimic (ThermoScientific) and after 24 hours spheroids were generated as previously described.[24] One hundred spheroids were generated per condition, collected after 24 hours and embedded in matrigel basement membrane matrix (BD Bioscience). Spheroids were monitored for 120 hours and photographs were taken on an Axiovert 100 microscope (Zeiss) using an AxioCam (Zeiss) and acquired using AxioVision software (Zeiss). To analyze average sprouts per spheroid, sprouts were counted using Adobe Photoshop CS2 (n = 60). Average sprout length was measured using the segmented lines tool in ImageJ (National Institutes of Health). Five sprouts were measured per spheroid (n = 20).

Embryo manipulation and in situ hybridization procedures

Zebrafish embryos were obtained by natural spawning of adult zebrafish. Embryos were raised and maintained at 28.5°C in system water and staged as described.[25] *Tg(kdrl:EGFP)*[26] and *Tg(fli1a:EGFP)*[27] lines were used to monitor blood vessel development. Antisense MOs (GeneTools) and miRNA mimics (Thermo Fischer Scientific) were injected into 1 to 4-cell-stage embryos. The MOs used in this work were MO1-*dll4* (5 ng),[6] *dll4*-TP$^{miR\text{-}30}$ 5′-TGTAAACAATCCAGAAAAAAAGATT-3′ (10 ng unless otherwise stated), *dll4*-TP^{control} 5′-ATAGCACTCTATTTAACTCTTTTAA-3′ (10ng unless otherwise stated), *kdr* MO[28] (4.5 ng), and *kdrl* MO[28] (4.5 ng). *dll4*-TP$^{miR\text{-}30}$ was designed so that the 3′ end binds to the miR-30 target site within the *dll4* 3′UTR, whereas the 5′ region binds to the downstream flanking sequence, as per Choi et al.[29] *dll4*-TP^{control} was designed so that it binds to another unrelated region of the *dll4* 3′UTR (596-620 nt), which is not predicted to contain any other miRNA binding sites, as per Choi et al.[29] miRNA mimics were injected in the quantities stated. In situ hybridization was performed as described.[30] RNA probes were labeled with digoxigenin (Roche) and detected using BM Purple (Roche). Images of in situ hybridizations were taken using a Nikon 1200F camera on a Nikon E1500 dissecting scope and acquired using ACT-1 software (Nikon). Fluorescent images of the *Tg(kdrl:EGFP)* and *Tg(fli1a:EGFP)* embryos were taken using an Axiocam (Zeiss) on an Axiovision Lumar V2 dissecting scope (Zeiss) and acquired using AxioVision Release 4.8.0 software. Figures were generated with Adobe Photoshop CS4.

Statistical and bioinformatics analysis

All experiments were performed in independent replicates and error bars correspond to SEM unless otherwise stated. Statistical significance (*P* value) was calculated with a 2-sided unpaired student *t* test unless otherwise stated. Processing and statistical analysis of the KLEC gene expression microarray (GEM) data (GSE17016) was performed using Bioconductor packages (*affy, limma*)[31] for the R programming language. GEM and RNAseq data for analysis of the correlation between *DLL4* and miR-30 in tumors compared with normal tissue were obtained from The Cancer Genome Atlas (www.cancergenome.nih.gov) data portal (https://tcga-data.nci.nih.gov/tcga). As data for each sample were individually processed rather than normalized as a batch and because data from different platforms and data types were analyzed, both the miRNA and gene expression data were scaled (ie, between 0 and 1) and centered (ie, approximately 0) before merging. For a full list of the sample numbers, data types, and platforms, please see supplemental Table 1 (available on the *Blood* Web site; see the Supplemental Materials link at the top of the online article).

Results

KSHV regulates expression of a miRNA family predicted to target *DLL4*

KSHV infection of endothelial cells, including LECs, is a tractable model to study aspects of endothelial cell biology.[14,32] *DLL4* is one of the most significantly up-regulated genes in KLECs.[12] We therefore examined the most down-regulated cellular miRNAs in KLECs to determine whether we could identify miRNAs that regulate *DLL4*.[20] We reanalyzed our microarray data with respect to down-regulated miRNAs and found that the miR-30 family is

Downloaded from http://ashpublications.org/blood/article-pdf/120/25/5063/1359076/zh805112005063.pdf by guest on 19 May 2024

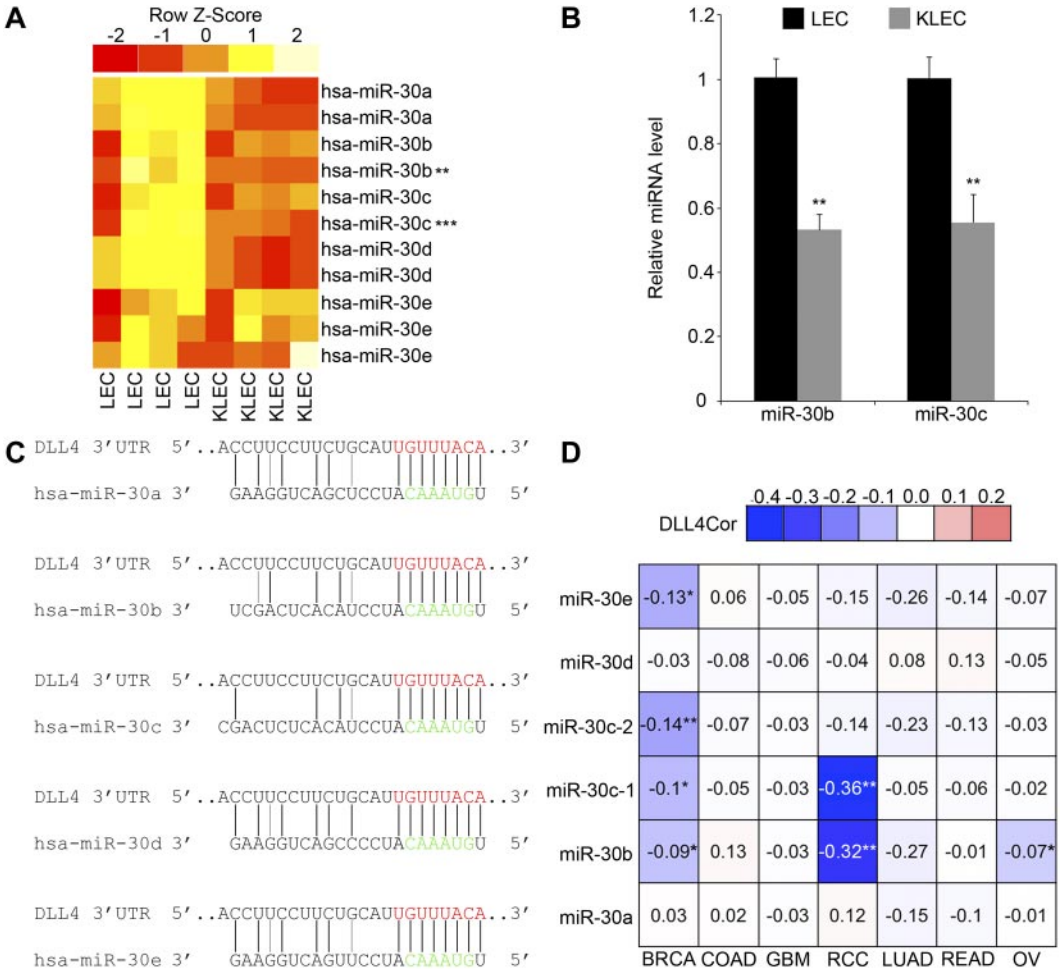

Figure 1. KSHV regulates expression of the miR-30 family, which is predicted to target *DLL4*. (A) Heatmap representing relative changes in expression of hsa-miR-30 family members in LECs after KSHV infection. Red and yellow denote low and high expression, respectively. Four replicates of LECs and KLECs are shown. Two to 3 probes are shown for each member of the miR-30 family. Probes for hsa-miR-30b and hsa-miR-30c showed significant changes in expression (**$Q < .01$; ***$Q < .001$). Original GEM data from Lagos et al.[20] (B) Down-regulation of miR-30b and miR-30c in KLECs, confirmed by qRT-PCR (means + SEM, n = 3). Expression is relative to LECs. Differences between LECs and KLECs were significant (**$P < .01$). (C) Complementarity between miR-30 family members and the *DLL4* 3′UTR. Black lines indicate canonical Watson and Crick base-pairing, gray lines indicate G:U wobbles. The predicted target site within the *DLL4* 3′UTR, positions 59 to 66, is shown in red; miR-30 seed region is shown in green. (D) Heatmap table displaying the correlation coefficient R between expression of *DLL4* and each member of the miR-30 family in the indicated tumor types. GEM and RNAseq data were obtained from The Cancer Genome Atlas (www.cancergenome.nih.gov) data portal (www.tcga-data.nci.nih.gov), as described in "Methods." Because of the large difference in the number of replicates for each tumor type, the significance of R was calculated for each mir-30 versus *DLL4* combination. The values and fill-in color indicate the degree of negative correlation. Nonsignificant correlations are grayed out; significant correlations are marked with an asterisk (*$P < .05$; **$P < .01$). Tumor types included are breast invasive carcinoma (BRCA), colon adenocarcinoma (COAD), glioblastoma multiforme (GBM), renal clear cell carcinoma (RCC), lung adenocarcinoma (LUAD), rectum adenocarcinoma (READ), and ovarian serous cystadenocarcinoma (OV).

down-regulated in KLECs 72 hours PI (Figure 1A). The most significantly suppressed probes corresponded to miR-30b and miR-30c and the microarray data were validated by qRT-PCR (Figure 1B). The mature miR-30c miRNA detected by the microarray can be produced from 2 distinct precursor hairpins (pre–miR-30c-1 and pre-miR-30c-2) and we confirmed down-regulation of both sources in KLECs (supplemental Figure 1A).

We used the TargetScan prediction algorithm to identify miR-30 targets and ranked them according to total context score.[33] We analyzed this list with respect to genes significantly altered in KLECs and discovered that the 3′UTR of *DLL4* scored favorably (total context score −0.39). TargetScan analysis of the *DLL4* 3′UTR sequence indicated that the miR-30 family is the best scoring miRNA for this 3′UTR (Figure 1C).

The miR-30 target site is an 8mer which is absolutely conserved within the *DLL4* 3′UTR across 22 species (supplemental Figure 1B). miRNAs are known to target Notch components during tumor development,[34] but a function for this cross-talk in tumorigenesis is unclear. Down-regulation of the miR-30 family is associated with enhanced tumorigenesis in breast cancer and anaplastic thyroid carcinoma.[35,36] However, an association between *DLL4* and miR-30 expression is not described. We analyzed mRNA and miRNA expression data from the The Cancer Genome Atlas (www.cancergenome.nih.gov), specifically studying angiogenic solid tumors. We found a significant negative correlation between 1 or more miR-30 family members and *DLL4* expression in breast adenocarcinoma, ovarian serous cystadenocarcinoma, and the highly angiogenic renal clear-cell carcinoma (Figure 1D). Most of the other tumors analyzed also displayed a negative correlation, although nonsignificant (Figure 1D).

miR-30b and miR-30c regulate DLL4

To validate our target predictions for miR-30b and 30c, we measured DLL4 expression after transfecting synthetic miR-30b and miR-30c mimics into LECs. DLL4 mRNA and protein levels

Downloaded from http://ashpublications.org/blood/article-pdf/120/25/5063/1359076/zh805112005063.pdf by guest on 19 May 2024

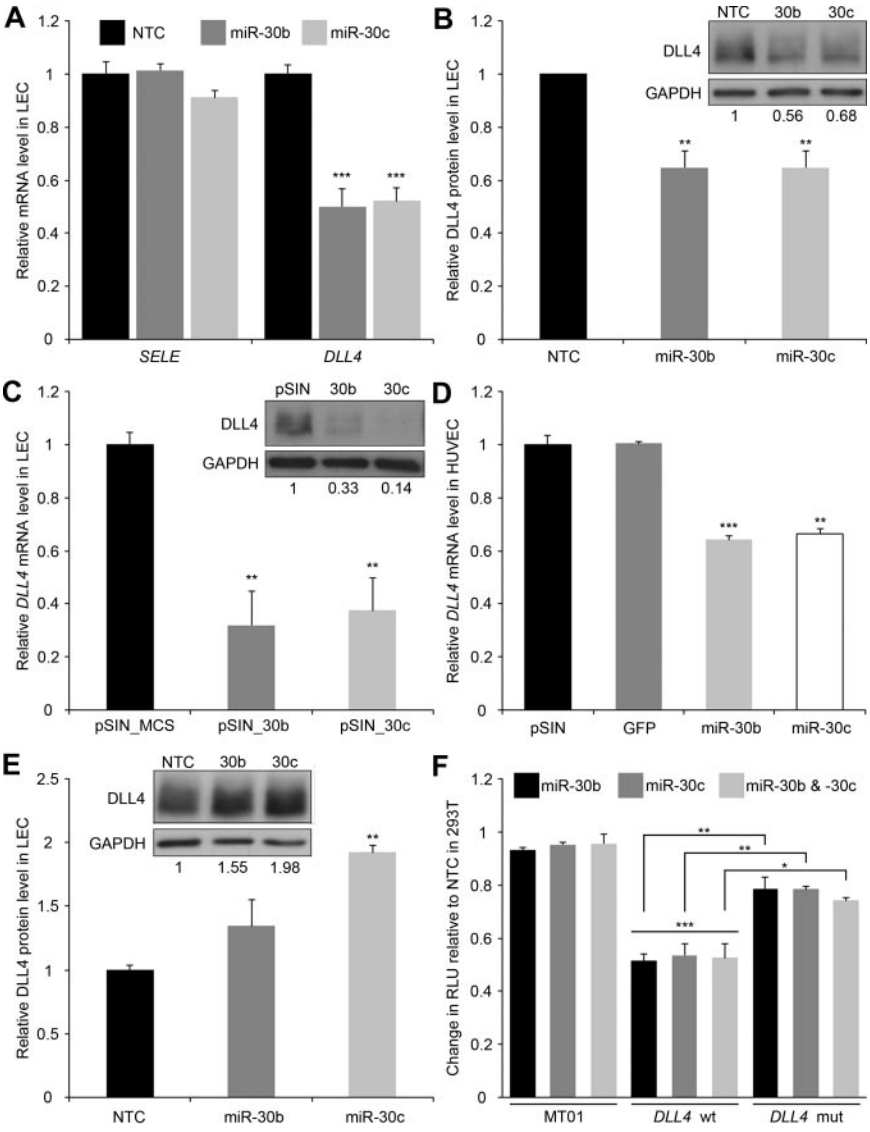

Figure 2. miR-30b and miR-30c regulate DLL4. *DLL4* (A-C-D) and *SELE* (A) mRNA expression, as measured by qRT-PCR, in LECs (A-C) or HUVECs (D) transfected with mimics (A) or infected with lentiviruses (C-D). DLL4 protein expression, as measured by Western blotting, in LECs transfected with mimics (B), infected with lentiviruses (C), or transfected with inhibitors (E). Values indicate intensity of DLL4 antibody ECL plus signal normalized to GAPDH antibody ECL signal. (A) Expression is relative to nontargeting control (NTC) mimic (means + SEM, n = 4). (B) Top panel: Representative Western blots, 20 minutes' exposure of DLL4 blot and 1-second exposure of GAPDH blot. Bottom panel: intensity is relative to NTC mimic (means + SEM, n = 3). (C) Top panel: Representative Western blots, 10 minutes' exposure of DLL4 blot and 1-second exposure of GAPDH blot. Bottom panel: expression is relative to empty vector, pSIN_MCS (means + SEM, n = 4). (D) Expression is relative to empty vector, pSIN_MCS (means + SEM, n = 3). (E) Top panel: representative Western blots, 30 minutes' exposure of DLL4 blot and 1-second exposure of GAPDH blot. Bottom panel: Intensity is relative to NTC inhibitor (means + SEM, n = 2). (F) Reporter assay indicating the response of WT or mutant (mut) *DLL4* 3′UTR to exogenous miR-30b and miR-30c (means + SEM, n = 3). Firefly expression was normalized to renilla expression to give the relative light units (RLU), which are shown relative to NTC mimic. MT01 is a control reporter, lacking a 3′UTR sequence but containing the firefly and renilla luciferase genes. Related statistically significant values are indicated by horizontal bars. In all panels, statistical significance denoted by $*P < .05$; $**P < .01$; $***P < .001$.

were significantly reduced in LECs expressing either mimic (Figure 2A-B) and this effect was dose-dependent (supplemental Figure 2A). Coexpression of miR-30b and miR-30c, at an equivalent total concentration, did not increase *DLL4* repression, suggesting that there are no additive or synergistic effects between these miR-30 family members (supplemental Figure 2A). These findings correspond with our target prediction studies, which indicate only 1 miR-30 target site on the *DLL4* 3′UTR (Figure 1C). Expression of an unrelated mRNA (*SELE*) was unchanged (Figure 2A), suggesting that the suppression of *DLL4* mRNA does not reflect a nonspecific effect of these mimics on global mRNA levels.[37]

As the highly stable mimics led to a supraphysiologic upregulation of miR-30 of more than 1000-fold (data not shown), we also used lentiviruses to overexpress miR-30 in its pre-miRNA form. Infection of LECs with lentiviruses expressing miR-30b or miR-30c (pSIN_30b or pSIN_30c) suppressed DLL4 (Figure 2C). This was confirmed in another type of endothelial cell, HUVECs (Figure 2D). We confirmed expression of the mature miRNAs in LECs and HUVECs transduced with these viruses (supplemental Figure 2B-C) and *DLL4* suppression increased with increasing viral copies per cell (supplemental Figure 2B). Conversely, transfection of hairpin inhibitors against miR-30b and miR-30c into LECs led to an increase in DLL4 protein levels (Figure 2E). Taken together, these data indicate that the miR-30 family regulates endogenous DLL4.

To confirm that these miRNAs act through the *DLL4* 3′UTR we used a vector with the luciferase coding sequence up-stream of the *DLL4* 3′UTR (*DLL4*_wt). We expressed this construct in the presence of miR-30b or miR-30c mimics (Figure 2F) and observed a 50% reduction in luciferase activity. The control vector maintained luciferase activity in the presence of exogenous miR-30, suggesting the changes in activity were because of the action of miR-30 on the *DLL4* 3′UTR. To confirm this we mutated the predicted miR-30 target site in the *DLL4* 3′UTR (supplemental Figure 2D) to prevent miRNA association (*DLL4*_mut). Luciferase activity was significantly increased to near-baseline levels (Figure 2F). These data indicate that miR-30 influences the expression of *DLL4* in endothelial cells by targeting a predicted site within its 3′UTR.

miR-30 targeting of *DLL4* influences endothelial cell behavior in vitro

DLL4 expression influences angiogenic pathways in endothelial cells and contributes to the angiogenic signature of KSHV-infected endothelial cells.[12,38] We therefore used KSHV-infection of LECs

Downloaded from http://ashpublications.org/blood/article-pdf/120/25/5063/1359076/zh805112005063.pdf by guest on 19 May 2024

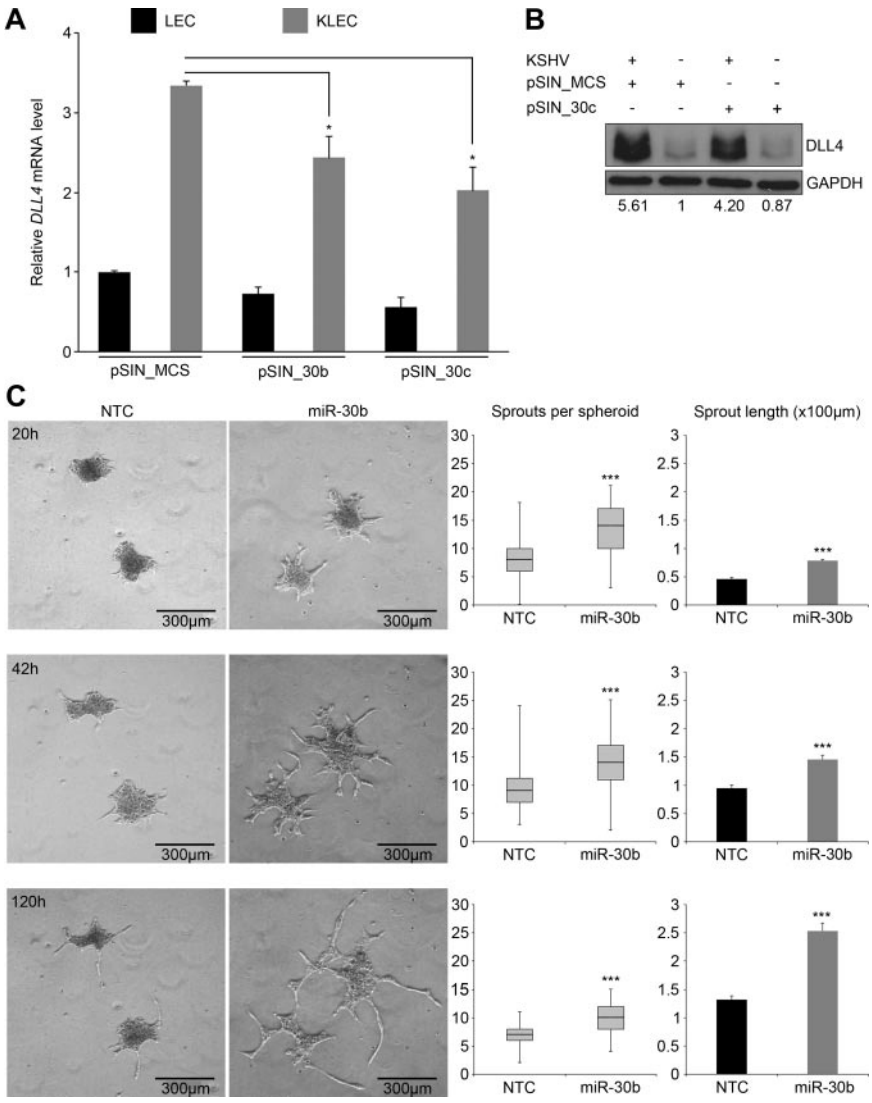

Figure 3. Regulation of DLL4 by miR-30b and miR-30c has relevance in pathophysiologic settings. (A) *DLL4* mRNA expression in LECs or KLECs infected with miR-30b and miR-30c–expressing lentiviruses measured by qRT-PCR (means + SEM, n = 3). Expression is relative to LECs infected with empty vector, pSIN_MCS. Differences between pSIN_MCS-infected and pSIN_30b/30c-infected KLECs were significant (*$P < .05$). (B) DLL4 protein expression in LECs measured by Western blotting. Values indicate intensity of DLL4 antibody ECL plus signal normalized to GAPDH antibody ECL signal and relative to KSHV−/pSIN_MCS+. (C) Left panels: Representative photographs at indicated time points of HUVEC spheroids embedded in matrigel. HUVECs were transfected with mimic before being induced to form spheroids. Photographs were taken on an Axiovert 100 microscope (Zeiss) using an AxioCam (Zeiss) at 5× magnification in phase contrast. Images were acquired using AxioVision (Zeiss). Middle panels: Quantification of total sprouts per spheroid (y-axis) at indicated time points (n = 60). Box plot indicates inter-quartile range, whiskers indicate total range, black line denotes median. Sprouts were counted using Adobe Photoshop CS2. The difference between NTC-transfected and miR-30b–transfected cells was significant (***$P < .001$). Right panels: Quantification of average sprout length (y-axis; means + SEM, n = 20). Average sprout length was measured using the segmented lines tool in Image J (National Institutes of Health) and are displayed on the y-axis as ×100 μm. Five sprouts were measured per spheroid. The difference between NTC-transfected and miR-30b–transfected cells was significant (***$P < .001$).

to investigate the effect of miR-30 on DLL4 levels. (Figure 3A-B). *DLL4* mRNA expression was increased 3-fold in KLECs compared with LECs and this induction was attenuated to 2-fold in KLECs expressing exogenous miR-30, suggesting that miR-30 can suppress *DLL4* levels in a dynamic system where it is normally up-regulated (Figure 3A). This was also reflected at the protein level where KSHV infection induced a 5-fold increase in DLL4 that was reduced to 4-fold in pSIN_30c transduced cells (Figure 3B). These findings reveal an additional miRNA-controlled layer of DLL4 regulation in human endothelial cells and are consistent with our previous work showing that activation of the extracellular-signal regulated kinase (ERK) pathway also drives DLL4 induction in KSHV-infected endothelial cells.[12]

During pathologic and physiologic angiogenesis, endothelial cells expressing DLL4 stimulate Notch signaling in adjacent cells and are specified as "tip" cells. Tip cells localize to the apex of the developing sprout, excluding the signal-receiving "stalk" cells, which contribute to the body of the developing vessel. Suppression of Notch signaling leads to excessive sprouting and multiple vessel branches because the tip cell phenotype is not restricted.[2] We used an in vitro model of sprouting angiogenesis to investigate whether *DLL4* targeting by miR-30b affected normal tip-cell behavior.[24] HUVECs expressing either miR-30b mimics or nontargeting control (NTC) were induced to form spheroids which were then embedded in matrigel. Those spheroids composed of miR-30b–overexpressing HUVECs displayed an increased propensity to form sprouts of greater length (Figure 3C) indicating that miR-30 overexpression promotes angiogenic sprouting. miR-30 mimics down-regulated *DLL4* mRNA in this cell type (supplemental Figure 3A-C).

Exogenous expression of miR-30 induces hyperbranching of intersegmental vessels in zebrafish

The developing zebrafish vasculature is an established model of angiogenic processes. Zebrafish Dll4 regulates angiogenic sprouting of ISVs and is detectable from 8 hours postfertilization (hpf) by RT-PCR[5]; using qRT-PCR, we observed *dll4* induction between 6 hpf and 12 hpf in zebrafish embryos (supplemental Figure 4A). Expression of miR-30b and miR-30c homologs is found during development and in the adult fish.[39] We observed a correlation between expression of miR-30 and *dll4* from 18 hpf to 30 hpf (supplemental Figure 4A) corresponding with the temporal window during which angiogenic sprouting occurs.[40]

Downloaded from http://ashpublications.org/blood/article-pdf/120/25/5063/1359076/zh805112005063.pdf by guest on 19 May 2024

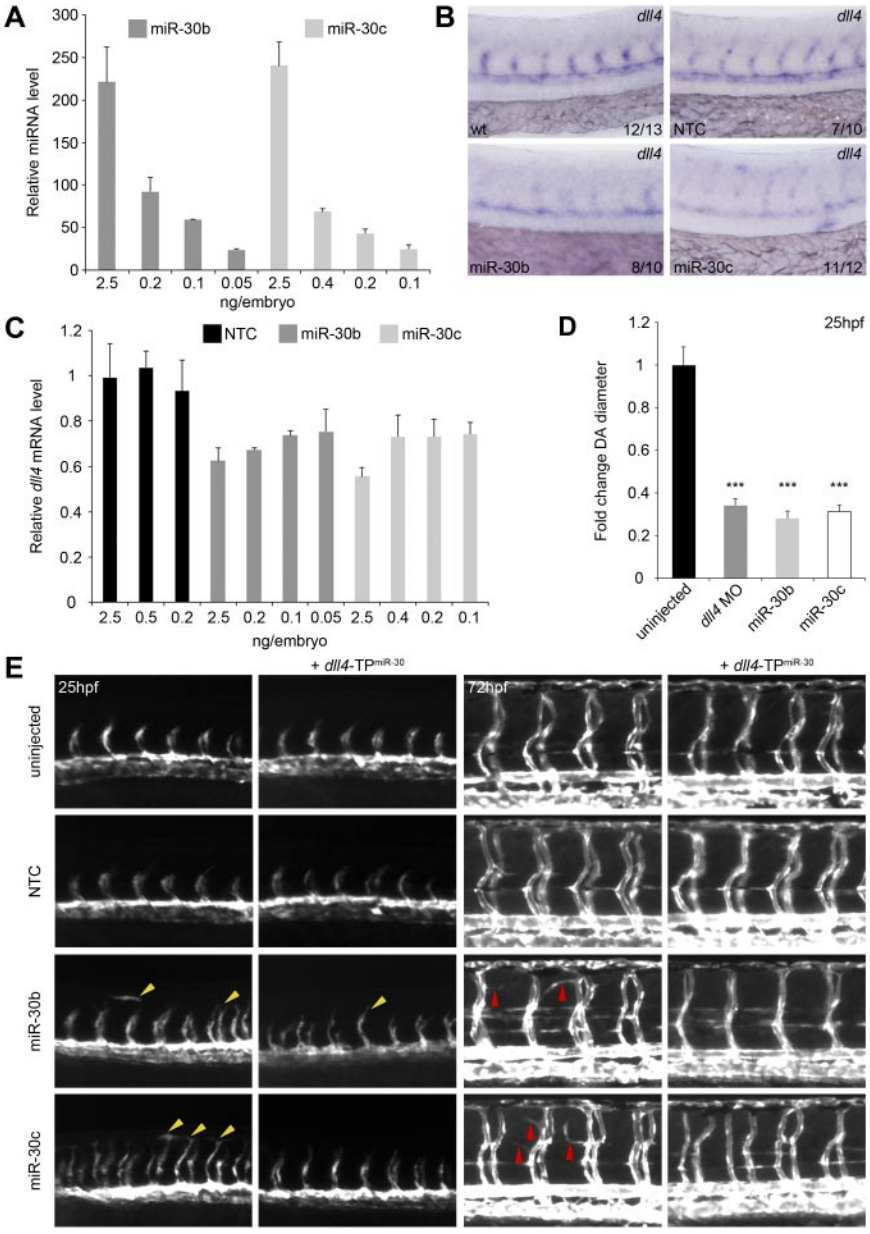

Figure 4. miR-30b and 30c regulate *dll4* expression and angiogenic sprouting in vivo. (A) Expression of miR-30 in whole zebrafish embryos after microinjection of miR-30 mimics at the 1- to 4-cell stage measured by qRT-PCR. Expression is relative to uninjected control embryos. Values indicate the amount of injected mimic. Error bars indicate SD of qRT-PCR experiment which was performed in triplicate. n = 1 but RNA was collected from 20 to 30 embryos per condition. (B) Representative in situ hybridization showing expression of *dll4* mRNA levels in the developing vasculature of WT zebrafish embryos and embryos injected with 0.05 ng (miR-30b) and 0.1 ng (miR-30c) miRNA mimics. Values indicate the number of embryos with the predominant, displayed phenotype versus the total number of embryos assayed. Images were taken using a Nikon 1200F camera on a Nikon E1500 dissecting microscope and acquired using ACT-1 software (Nikon). Images were cropped using Adobe Photoshop CS4. (C) Expression of *dll4* mRNA in whole zebrafish embryos after microinjection with miR-30 mimics measured by qRT-PCR. Expression is relative to uninjected control embryos. Values indicate amount of injected mimic. Error bars indicate SD of qRT-PCR which was performed in triplicate. n = 1 but RNA was collected from 20 to 30 embryos per condition. (D) DA diameter in embryos injected with *dll4* MO or miR-30 mimic relative to uninjected embryos (means + SEM, n = 3). Six DA measurements were made per embryo using Adobe Photoshop CS4. Differences between uninjected embryos and embryos injected with *dll4* MO or miR-30 mimics were significant (***$P < .001$). (E) Trunk vasculature in uninjected *Tg(kdrl:EGFP)* embryos or embryos injected with the indicated miRNA mimic and/or TP. Left panels: Advanced sprouting and aberrant endothelial cell migration (yellow arrowheads) at 25 hpf. Right panels: Increased branching of the ISVs (red arrowheads) at 72 hpf. Fluorescent images were taken using an Axiocam (Zeiss) on an Axiovision Lumar V12 dissecting microscope (Zeiss) and acquired using AxioVision v4.8 software. Images were cropped and arrowheads were added using Adobe Photoshop CS4.

These temporally coincident changes in *dll4* and miR-30 suggest a functional interaction that may contribute to tight control of Dll4 expression during vascular development. We investigated this relationship by increasing miR-30 expression through microinjection of miR-30 mimics. To reduce nonspecific effects of exogenous miR-30, microinjected mimic was titrated to levels where overall embryo morphology was normal and miR-30 expression was detectable at a physiologically relevant level (Figure 4A). We considered an up-regulation of 20- to 25-fold to be within physiologic levels, as changes of this magnitude are seen for individual miRNAs during zebrafish development.[41] We confirmed the down-regulation of *dll4* expression in the vasculature by in situ hybridization (Figure 4B). *dll4* expression titrated with levels of miR-30 and was reduced by 20% to 30% compared with control embryos at the lowest mimic concentrations (Figure 4C). These data indicate that *dll4* mRNA levels can be disrupted in vivo by exogenous expression of miR-30.

It was previously shown that *dll4* silencing using MOs induces excessive ISV branching.[5,6] We investigated the effect of reduced *dll4* expression by miR-30 on endothelial cell behavior in *Tg(kdrl:EGFP)* zebrafish, using *dll4* MO-injected embryos as a positive control (Figure 4E, supplemental Figure 4B). Compared with uninjected control embryos, we found that embryos expressing miR-30b or miR-30c mimics showed vessel-free, hyper-migratory endothelial cells, ISVs at a more advanced stage of sprouting and premature dorsal longitudinal anastomotic vessel (DLAV) formation at 25 hpf (Figure 4E, supplemental Figure 4B left panels yellow arrowheads). With increasing amounts of miR-30 mimic, a higher percentage of embryos displayed advanced sprouting and a greater proportion of these exhibited premature DLAV formation and hyper-migratory behavior (supplemental Figure 5A). This phenotype was also present in *dll4* MO-injected embryos (supplemental Figure 4B), suggesting that miR-30 overexpression phenocopies the *dll4* morphant phenotype. At 25 hpf, the diameter of the DA was significantly reduced in *dll4* morphants and in miR-30–overexpressing embryos compared with WT embryos (Figure 4D). This reduction in vessel diameter concurs with previous work showing that DLL4 up-regulation in tumors correlates with vessel

Downloaded from http://ashpublications.org/blood/article-pdf/120/25/5063/1359076/zh805112005063.pdf by guest on 19 May 2024

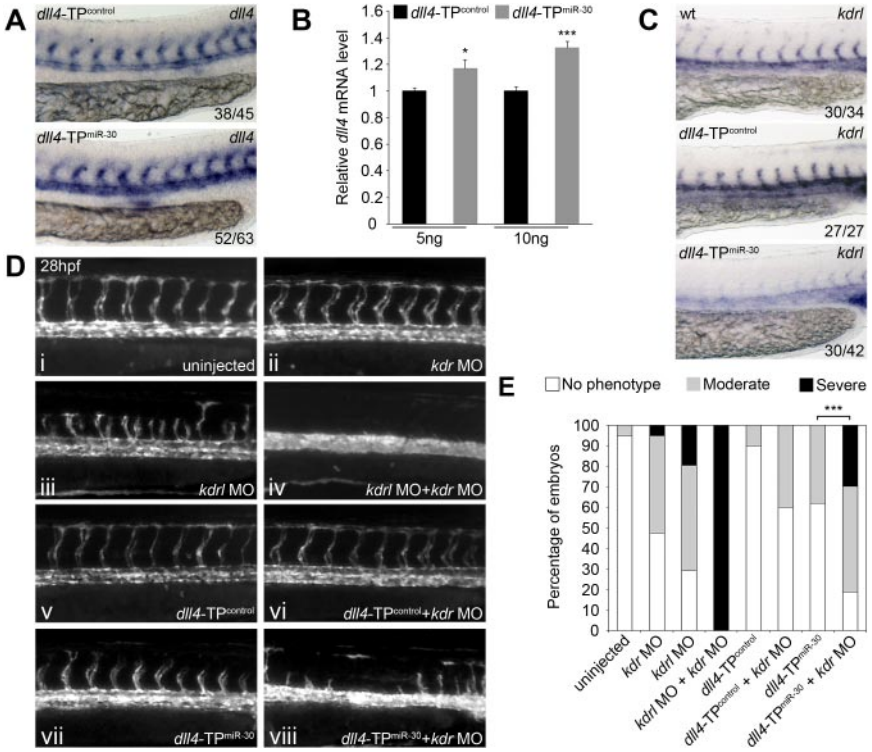

Figure 5. Loss of *dll4* regulation by miR-30 synergizes with partial Vegfa signaling knockdown to block angiogenesis. (A) Representative in situ hybridization showing expression of *dll4* mRNA in the developing vasculature of zebrafish embryos injected with 10 ng of the indicated TP. Values indicated the number of embryos with the predominant, displayed phenotype versus the total number of embryos assayed. Images were taken using a Nikon 1200F camera on a Nikon E1500 dissecting microscope and acquired using ACT-1 software (Nikon). Images were cropped using Adobe Photoshop CS4. (B) Expression of *dll4* mRNA in whole zebrafish embryos after microinjection of *dll4*-TP$^{miR\text{-}30}$ measured by qRT-PCR (means + SEM, n = 5). Expression is relative to embryos injected with *dll4*-TP^{control}. Values indicate the amount of injected TP as ng/embryo. Differences between *dll4*-TP^{control} and *dll4*-TP$^{miR\text{-}30}$ injected embryos were significant (*$P < .05$, ***$P < .001$). (C) Trunk vasculature in uninjected *Tg(fli1a:EGFP)* embryos or embryos injected with the indicated MO and/or TP at 28 hpf. Fluorescent images were taken using an Axiocam (Zeiss) on an Axiovision Lumar V12 dissecting microscope (Zeiss) and acquired using AxioVision v4.8 software. Images were cropped using Adobe Photoshop CS4. (D) Quantification of ISV sprouting defects after injection of the MOs and/or TPs indicated. Columns are the average of 2 independent experiments with 15 to 30 embryos counted per sample per experiment. Moderate phenotype: embryos lacking 1 ISV but with a minimum of 6 ISVs. Severe phenotype: embryos with 5 or less ISVs. To determine statistical significance, each observation of no phenotype, moderate phenotype and severe phenotype was given the value 0, 1, and 2, respectively, and then a Wilcoxon rank-sum test was performed. The difference between embryos injected with *dll4*-TP$^{miR\text{-}30}$ and embryos injected with *dll4*-TP$^{miR\text{-}30}$ + *kdr* MO was significant (***$P < .001$). Embryos were examined using an Axiovision Lumar V2 dissecting microscope (Zeiss) for quantification to be performed. (E) Representative in situ hybridization showing expression of *kdrl* mRNA in the developing vasculature of a WT embryo and embryos injected with 10 ng of the indicated TP. Values indicated the number of embryos with the predominant, displayed phenotype versus the total number of embryos assayed. Images were taken using a Nikon 1200F camera on a Nikon E1500 dissecting microscope and acquired using ACT-1 software (Nikon). Images were cropped using Adobe Photoshop CS4.

maturation and size.[9,42] At 72 hpf, excessive ISV branching (Figure 4E, supplemental Figure 4B right panels red arrowheads) was found in embryos expressing miR-30b and 30c mimics, comparable with the branching induced by *dll4* knockdown (supplemental Figure 4B red arrowheads; Leslie et al[5]). This phenotype titrated with increasing amounts of miR-30: the higher the amount of mimic injected, the greater the number of branches from the ISVs (supplemental Figure 5B).

To confirm that the miR-30 family targeted *dll4* in vivo, embryos were coinjected with a target protector MO (TP) designed to bind to a region within the *dll4* 3′UTR containing the miR-30 target site (*dll4*-TP$^{miR\text{-}30}$).[29] Coinjection of *dll4*-TP$^{miR\text{-}30}$ with miR-30b or miR-30c mimics led to a partial rescue of the miR-30–induced ISV hyperbranching (Figure 4E), with the advanced sprouting phenotype being reduced by approximately one-half in coinjected embryos (supplemental Figure 4C). These findings indicate that *dll4* down-regulation is a significant contributing factor to the advanced sprouting and excessive branching phenotypes observed. These data suggest that miR-30 can regulate endothelial cell behavior in vivo and that the targeting of *dll4* by miR-30 is functionally relevant during vascular development.

Increased *dll4* expression synergizes with partial loss of VegfA signaling to inhibit angiogenesis

To investigate the endogenous role of miR-30 in the regulation of *dll4*, we injected *dll4*-TP$^{miR\text{-}30}$ or *dll4*-TP^{control} alone and examined *dll4* expression at 28 hpf. Consistent up-regulation of *dll4* in *dll4*-TP$^{miR\text{-}30}$ injected embryos was observed by in situ hybridization (Figure 5A) and qRT-PCR (Figure 5B). When *Tg(fli1a:EGFP)* zebrafish were injected with *dll4*-TP$^{miR\text{-}30}$ alone, we observed an increase in the percentage of embryos with shorter or missing ISVs at 28 hpf (Figure 5Cvii,D), suggesting that elevating *dll4* levels partially blocked ISV angiogenesis.

Notch signaling via DLL4 negatively regulates expression of VEGFR2, the receptor through which VEGFA signals. Microarray and qRT-PCR analyzes of HUVECs transduced with empty vector and DLL4-encoding retroviruses have previously shown that *VEGFR2* is down-regulated in DLL4-expressing HUVECs,[38] whereas HUVECs cultured on recombinant DLL4-coated plates display reduced VEGFR2 protein levels.[38] This down-regulation is known to be caused by DLL4 signaling through NOTCH as HUVECs cultured on recombinant DLL4-coated plates in the presence of the γ-secretase inhibitor DAPT did not show VEGFR2

Downloaded from http://ashpublications.org/blood/article-pdf/120/25/5063/1359076/zh805112005063.pdf by guest on 19 May 2024

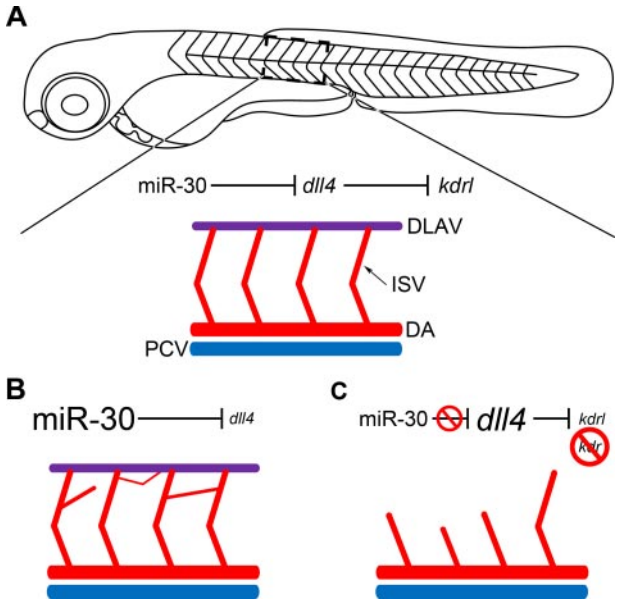

Figure 6. Schematic representation of the functional consequences of *DLL4* targeting by miR-30. (A) A zebrafish embryo at 72 hpf is depicted. A section of the intersegmental vessels (ISV) has been enlarged. The dorsal aorta (DA) and posterior cardinal vein (PCV) have also been depicted in red and blue, respectively. The dorsal longitudinal anastomotic vessel (DLAV) is shown in purple. (B) When miR-30 is overexpressed, *dll4* is down-regulated and a deregulated network of intersegmental vessels forms as the tip cell phenotype is not restricted and excessive sprouting occurs. (C) When miR-30 regulation of *dll4* is blocked using a target protector, *dll4* is up-regulated, and consequently *kdrl* expression is reduced. When combined with *kdr* knockdown, the restriction of tip cell specification and inhibition of Vegfa signaling which ensues prevents normal intersegmental vessel sprouting and the DLAV does not form.

down-regulation.[38] The enzyme γ-secretase is required for the final stage of NOTCH receptor cleavage during Notch signaling.[1] Zebrafish possess 2 functional orthologs of *VEGFR2*: *kinase insert domain receptor* (*kdr*) and *kinase insert domain receptor like* (*kdrl*).[43] Knockdown of *kdrl* partially blocks Vegfa signaling and decreases ISV sprouting from the DA in *Tg(fli1a:EGFP)* embryos (Figure 5Ciii,D).[28] Kdrl acts synergistically with Kdr to mediate Vegfa signaling.[28] Simultaneous knockdown of *kdr* and *kdrl* causes complete loss of ISVs,[28] a phenotype which we successfully recapitulated (Figure 5Civ,D). When investigating potential changes in downstream targets of Dll4 by in situ hybridization, we noted that *kdrl* was down-regulated on *dll4*-TP^{miR-30} injection (Figure 5E). This suggested that the miR-30 family is indirectly regulating the levels of Vegfa signaling by negatively regulating *dll4* expression which subsequently increases *kdrl* expression. Indeed, coinjection of *dll4*-TP^{miR-30} with the *kdr* MO (Figure 5Cviii) resulted in increased loss of ISV sprouting compared with *dll4*-TP^{miR-30} (Figure 5Cvii) or *kdr* MO alone (Figure 5Cii), as quantified in Figure 5D. We propose that this is caused by impairment in Vegfa signaling because of the combined down-regulation of *kdr*, by the *kdr* MO, and *kdrl*, by the *dll4*-TP^{miR-30} through *dll4* up-regulation. These data suggest that tight regulation of *dll4* levels by the miR-30 family confers robustness to the Vegfa-mediated angiogenesis process in vivo.

In conclusion, we show that miR-30 acts to fine tune *dll4* levels during zebrafish vascular development, allowing sprouting angiogenesis to occur to the required extent (Figure 6A). When miR-30 is overexpressed, *dll4* is down-regulated so tip cell fate is not restricted; this results in excessive branching from the ISVs (Figure 6B). If the interaction between miR-30 and *dll4* is inhibited, the latter is up-regulated and consequently there is a reduction in *kdrl* expression (Figure 6C). If *kdr* is also suppressed, the subsequent lack of Vegfa signaling results in impaired ISV sprouting (Figure 6C).

Discussion

The 5 members of the miR-30 family all share the same seed sequence and are encoded by 6 genes located on human chromosomes 1, 6, and 8. This level of redundancy would suggest a critical functional role for this miRNA family. Members of the miR-30 family have been implicated in osteoblast differentiation,[44] adipogenesis,[45] epithelial-to-mesenchymal transition (EMT),[35,46] Xenopus pronephros development,[47] cellular senescence,[48] myocardial matrix remodeling,[49] and cancer.[35,36] Genes that have been identified as targets of 1 or more miR-30 family members include snail homolog 1 (drosophila; *SNAI1*)[46]; *LIM homeobox 1* (*lhx1*)[47]; B-cell lymphoma 6 (*BCL6*)[50]; v-myb myeloblastosis viral oncogene homolog (avian)–like 2 (*MYBL2*)[48]; and runt-related transcription factor 2 (*RUNX2*).[45] Our study is the first to identify and validate *DLL4* as a target of miR-30 and to demonstrate a key role for miR-30 in angiogenesis.

For sprouting angiogenesis to occur successfully a balance must be maintained between the number of tip cells, which lead the nascent sprouts, and stalk cells which will make up the endothelium of the new vessel.[2] DLL4 plays a crucial role in regulating the ratio of tip cells to stalk cells. Specifically, expression of DLL4 by the tip cells stimulates Notch signaling in the adjacent cells, thereby maintaining stalk cell identity and restricting tip-cell specification.[4] When DLL4 signaling or expression is inhibited, tip-cell specification is not controlled, leading to excessive sprouting from existing vessels. This can be seen during zebrafish ISV development, when knockdown of *dll4* causes the formation of an aberrant network of interconnected branches.[5] It is also relevant to the control of tumor vasculature as the use of blocking antibodies against DLL4 has been shown to promote angiogenesis, but the increased tumor vascularity is leaky and hence nonproductive, leading to the inhibition of tumor growth.[10,11] We hypothesized that *DLL4* is not only regulated at the transcriptional level but that its expression is subject to fine-tuning by posttranscriptional mechanisms, such as miRNAs, to maintain optimal levels for successful angiogenesis.

We used KSHV infection of LECs as a model with which to study *DLL4* regulation, as *DLL4* is one of the most significantly up-regulated genes in KLECs.[12] We observed significant down-regulation of miR-30b and miR-30c in KLECs, which was of interest given that the miR-30 family was predicted to target *DLL4* via a highly conserved 8mer target site within the 3′UTR. The simultaneous up-regulation of *DLL4* and suppression of miR-30 in KLECs suggested a possible regulatory relationship between *DLL4* and miR-30 in endothelial cells. This was further supported by our observation that *DLL4* and miR-30 are negatively correlated in several tumor types that are moderately or highly angiogenic. We confirmed that *DLL4* is a target of miR-30 and that miR-30 actively regulates endogenous *DLL4* in human vascular and lymphatic endothelial cells in vitro and during zebrafish vascular development in vivo. We have shown, both in vitro and in vivo, that miR-30 controls *DLL4* expression through a specific site within the *DLL4* 3′UTR. This regulation is also relevant to oncogenic virus infection, as the up-regulation of DLL4, which is normally seen in KLECs, was attenuated by the application of exogenous miR-30.

Our study has revealed a functional role for miR-30 in the regulation of angiogenesis via *DLL4* targeting. Overexpression of

Downloaded from http://ashpublications.org/blood/article-pdf/120/25/5063/1359076/zh805112005063.pdf by guest on 19 May 2024

miR-30 in endothelial cells promotes angiogenic sprouting in vitro. The introduction of exogenous miR-30 into zebrafish embryos led to aberrant migration of endothelial cells and longer sprouts at 25 hpf which developed into excessive ISV branching at 72 hpf, phenotypes also observed after *dll4* knockdown. We show that the excessive vascular sprouting caused by miR-30 overexpression was by way of *dll4* targeting through the use of a TP, specific to the miR-30 target site within the *dll4* 3′UTR. Recently it has been shown that knockdown of miR-27b causes defective vascular sprouting in developing zebrafish embryos.[18] Rescue studies using knockdown of *dll4* and *spry2* implicated these 2 targets as the causative agents of this phenotype; however, TP studies were not used to fully delineate the respective roles of *dll4* and *spry2*. The angiogenesis inhibitor *SEMA6A* has also been identified as a target of miR-27b,[19] and could account for the phenotype seen on miR-27b inhibition in zebrafish embryos.

The TP also provided us with a useful tool with which to explore the endogenous role of miR-30 during zebrafish vascular development. We used it to specifically block the interaction of miR-30 with *dll4* during development, while still allowing miR-30 to interact with its other targets. We have shown that inhibiting the normal control of *dll4* by miR-30 elevates *dll4* levels, which partially blocks ISV angiogenesis. This would suggest that during normal ISV sprouting miR-30 is actively suppressing *dll4*, helping to maintain tight control of *dll4* expression and hence angiogenesis. However, further investigations revealed a more intricate regulatory pathway. VEGFR2 expression has been shown to be inhibited by Notch signaling via DLL4.[38] When *dll4* levels were increased using the TP, we observed down-regulation of *kdrl*, a functional ortholog of *VEGFR2*.[43] Vegfa signaling in zebrafish is mediated through the synergistic action of Kdrl and another Vegfa receptor, Kdr.[28] When injection of *dll4*-TP$^{miR\text{-}30}$ was combined with knockdown of *kdr,* ISV sprouting was moderately to severely inhibited in the majority of embryos, as seen when the expression of both *kdrl* and *kdr* is blocked using MOs.[28] This work has therefore revealed that the miR-30 family indirectly regulates Vegfa signaling by controlling *dll4* expression and that this regulatory axis confers robustness to Vegfa-mediated angiogenesis.

We have identified and validated *DLL4* as a novel target of the miR-30 family and demonstrated the important role of these miRNAs during sprouting angiogenesis. We show that miR-30 regulates vascular development in vivo and provides robustness to Vegfa signaling by indirectly influencing *kdrl* expression. Our findings indicate that the manipulation of miR-30 in the setting of pathologic vascularization could represent a new therapeutic approach.

Acknowledgments

The authors thank Prof A. Harris and Dr E. Bridges for advising on the 3D spheroid in vitro angiogenesis assay.

This work was funded by a United Kingdom MRC PhD Studentship (G.B.), an MRC Program Grant (C.B. and D.L.), a BHF project grant (R.M. and R.P.), an MRC Unit Grant (R.M. and R.P.), and by Cancer Research UK (S.H., V.E., and C.B.).

Authorship

Contribution: G.B. designed and performed the experiments, analyzed the data, and wrote the paper; R.M. designed and performed the zebrafish experiments and assisted in preparation of the paper; S.H. provided the bioinformatics analysis and statistical assistance; V.E. designed experiments and assisted with paper preparation; D.L. performed the miRNA microarray and assisted with paper preparation; D.G. performed some of the KSHV experiments; R.P. assisted with paper preparation; and C.B. designed the experiments, supervised the project, and wrote the paper.

Conflict-of-interest disclosure: G.B., V.E., and C.B., are joint inventors on a patent application for *DLL4* targeting by the miR-30 family, which was filed at the UKPTO on 09.02.11, application No. 1102283.7. The remaining authors declare no competing financial interests.

Correspondence: Chris Boshoff, Cancer Research UK Viral Oncology Group, UCL Cancer Institute, University College London, London, WC1E 6BT, United Kingdom; e-mail: c.boshoff@ucl.ac.uk.

References

1. Gridley T. Notch signaling in the vasculature. In: Raphael K, ed. Current Topics in Developmental Biology Notch Signaling. Vol 92. Waltham, MA: Academic Press; 2010:277-309.
2. Phng LK, Gerhardt H. Angiogenesis: a team effort coordinated by Notch. *Dev Cell.* 2009;16(2):196-208.
3. Gale NW, Dominguez MG, Noguera I, et al. Haploinsufficiency of delta-like 4 ligand results in embryonic lethality due to major defects in arterial and vascular development. *Proc Natl Acad Sci U S A.* 2004;101(45):15949-15954.
4. Hellström M, Phng LK, Hofmann JJ, et al. Dll4 signalling through Notch1 regulates formation of tip cells during angiogenesis. *Nature.* 2007; 445(7129):776-780.
5. Leslie JD, Ariza-McNaughton L, Bermange AL, McAdow R, Johnson SL, Lewis J. Endothelial signalling by the Notch ligand Delta-like 4 restricts angiogenesis. *Development.* 2007;134(5):839-844.
6. Siekmann AF, Lawson ND. Notch signalling limits angiogenic cell behaviour in developing zebrafish arteries. *Nature.* 2007;445(7129):781-784.
7. Jubb AM, Soilleux EJ, Turley H, et al. Expression of vascular Notch ligand Delta-like 4 and inflammatory markers in breast cancer. *Am J Pathol.* 2010;176(4):2019-2028.
8. Patel NS, Li JL, Generali D, Poulsom R, Cranston DW, Harris AL. Up-regulation of Delta-like 4 ligand in human tumor vasculature and the role of basal expression in endothelial cell function. *Cancer Res.* 2005;65(19):8690-8697.
9. Patel NS, Dobbie MS, Rochester M, et al. Up-regulation of endothelial Delta-like 4 expression correlates with vessel maturation in bladder cancer. *Clin Cancer Res.* 2006;12(16):4836-4844.
10. Noguera-Troise I, Daly C, Papadopoulos NJ, et al. Blockade of Dll4 inhibits tumour growth by promoting non-productive angiogenesis. *Nature.* 2006;444(7122):1032-1037.
11. Ridgway J, Zhang G, Wu Y, et al. Inhibition of Dll4 signalling inhibits tumour growth by deregulating angiogenesis. *Nature.* 2006;444(7122):1083-1087.
12. Emuss V, Lagos D, Pizzey A, Gratrix F, Henderson SR, Boshoff C. KSHV manipulates Notch signaling by DLL4 and JAG1 to alter cell cycle genes in lymphatic endothelia. *PLoS Pathog.* 2009;5(10):e1000616.
13. Liu R, Li X, Tulpule A, et al. KSHV-induced notch components render endothelial and mural cell characteristics and cell survival. *Blood.* 2010; 115(4):887-895.
14. Wang HW, Trotter MWB, Lagos D, et al. Kaposi sarcoma herpes virus-induced cellular reprogramming contributes to the lymphatic endothelial gene expression in Kaposi sarcoma. *Nat Genet.* 2004;36(7):687-693.
15. Carthew RW, Sontheimer EJ. Origins and mechanisms of miRNAs and siRNAs. *Cell.* 2009;136(4): 642-655.
16. Croce CM. Causes and consequences of microRNA dysregulation in cancer. *Nat Rev Genet.* 2009;10(10):704-714.
17. Wang S, Olson EN. AngiomiRs–key regulators of angiogenesis. *Curr Opin Genet Dev.* 2009;19(3): 205-211.
18. Biyashev D, Veliceasa D, Topczewski J, et al. miR-27b controls venous specification and tip cell fate. *Blood.* 2012;119(11):2679-87.
19. Urbich C, Kaluza D, Frömel T, et al. MicroRNA-27a/b controls endothelial cell repulsion and angiogenesis by targeting semaphorin 6A. *Blood.* 2012;119(6):1607-1616.
20. Lagos D, Pollara G, Henderson S, et al. miR-132

Downloaded from http://ashpublications.org/blood/article-pdf/120/25/5063/1359076/zh805112005063.pdf by guest on 19 May 2024

regulates antiviral innate immunity through suppression of the p300 transcriptional co-activator. *Nat Cell Biol.* 2010;12(5):513-519.

21. Lewis BP, Shih IH, Jones-Rhoades MW, Bartel DP, Burge CB. Prediction of mammalian microRNA targets. *Cell.* 2003;115(7):787-798.
22. Vieira J, O'Hearn P, Kimball L, Chandran B, Corey L. Activation of Kaposi's sarcoma-associated herpes virus (Human Herpes virus 8) lytic replication by human cytomegalovirus. *J Virol.* 2001;75(3):1378-1386.
23. Vart RJ, Nikitenko LL, Lagos D, et al. Kaposi's sarcoma-associated herpes virus-encoded interleukin-6 and G-protein-coupled receptor regulate angiopoietin-2 expression in lymphatic endothelial cells. *Cancer Res.* 2007;67(9):4042-4051.
24. Weber H, Claffey J, Hogan M, Pampillón C, Tacke M. Analyses of Titanocenes in the spheroid-based cellular angiogenesis assay. *Toxicol In Vitro.* 2008;22(2):531-534.
25. Westerfield M. The zebrafish book; a guide for laboratory use of zebrafish (Brachydanio rerio). Eugene, OR: University of Oregon Press; 1993.
26. Beis D, Bartman T, Jin SW, et al. Genetic and cellular analyses of zebrafish atrioventricular cushion and valve development. *Development.* 2005; 132(18):4193-4204.
27. Lawson ND, Weinstein BM. In vivo imaging of embryonic vascular development using transgenic zebrafish. *Dev Biol.* 2002;248(2):307-318.
28. Bahary N, Goishi K, Stuckenholz C, et al. Duplicate VegfA genes and orthologues of the KDR receptor tyrosine kinase family mediate vascular development in the zebrafish. *Blood.* 2007; 110(10):3627-3636.
29. Choi WY, Giraldez AJ, Schier AF. Target protectors reveal dampening and balancing of nodal agonist and antagonist by miR-430. *Science.* 2007;318(5848):271-274.
30. Jowett T, Yan Y-L. Double fluorescent in situ hybridization to zebrafish embryos. *Trends Genet.* 1996;12(10):387-389.
31. Smyth GK. Linear models and empirical bayes methods for assessing differential expression in microarray experiments. *Stat Appl Genet Mol Biol.* 2004;3:article 3.
32. Mesri EA, Cesarman E, Boshoff C. Kaposi's sarcoma and its associated herpes virus. *Nat Rev Cancer.* 2010;10(10):707-719.
33. Grimson A, Farh KK-H, Johnston WK, Garrett-Engele P, Lim LP, Bartel DP. MicroRNA targeting specificity in mammals: determinants beyond seed pairing. *Mol Cell.* 2007;27(1):91-105.
34. Wang Z, Li Y, Kong D, Ahmad A, Banerjee S, Sarkar FH. Cross-talk between miRNA and Notch signaling pathways in tumor development and progression. *Cancer Lett.* 2010;292(2):141-148.
35. Braun J, Hoang-Vu C, Dralle H, Hüttelmaier S. Downregulation of microRNAs directs the EMT and invasive potential of anaplastic thyroid carcinomas. *Oncogene.* 2010;29(29):4237-4244.
36. Yu F, Deng H, Yao H, Liu Q, Su F, Song E. Mir-30 reduction maintains self-renewal and inhibits apoptosis in breast tumor-initiating cells. *Oncogene.* 2010;29(29):4194-4204.
37. Khan AA, Betel D, Miller ML, Sander C, Leslie CS, Marks DS. Transfection of small RNAs globally perturbs gene regulation by endogenous microRNAs. *Nat Biotechnol.* 2009;27(6):549-555.
38. Harrington LS, Sainson RCA, Williams CK, et al. Regulation of multiple angiogenic pathways by Dll4 and Notch in human umbilical vein endothelial cells. *Microvasc Res.* 2008;75(2):144-154.
39. Wienholds E, Kloosterman WP, Miska E, et al. MicroRNA expression in zebrafish embryonic development. *Science.* 2005;309(5732):310-311.
40. Ellertsdóttir E, Lenard A, Blum Y, et al. Vascular morphogenesis in the zebrafish embryo. *Dev Biol.* 2010;341(1):56-65.
41. Chen PY, Manninga H, Slanchev K, et al. The developmental miRNA profiles of zebrafish as determined by small RNA cloning. *Genes Dev.* 2005; 19(11):1288-1293.
42. Li JL, Sainson RCA, Shi W, et al. Delta-like 4 Notch ligand regulates tumor angiogenesis, improves tumor vascular function, and promotes tumor growth in vivo. *Cancer Res.* 2007;67(23): 11244-11253.
43. Bussmann J, Lawson N, Zon L, Schulte-Merker S, Zebrafish Nomenclature Committee. Zebrafish VEGF receptors: a guideline to nomenclature. *PLoS Genet.* 2008;4(5):e1000064.
44. Wu T, Zhou H, Hong Y, Li J, Jiang X, Huang H. miR-30 family members negatively regulate osteoblast differentiation. *J Biol Chem.* 2012; 287(10):7503-7511.
45. Zaragosi L-E, Wdziekonski B, Le Brigand K, et al. Small RNA sequencing reveals miR-642a–3p as a novel adipocyte-specific microRNA and miR-30 as a key regulator of human adipogenesis. *Genome Biol.* 2011;12(7):R64.
46. Zhang J, Zhang H, Liu J, et al. miR-30 inhibits TGF-β1-induced epithelial-to-mesenchymal transition in hepatocyte by targeting Snail1. *Biochem Biophys Res Commun.* 2012;417(3):1100-1105.
47. Agrawal R, Tran U, Wessely O. The miR-30 miRNA family regulates Xenopus pronephros development and targets the transcription factor Xlim1/Lhx1. *Development.* 2009;136(23):3927-3936.
48. Martinez I, Cazalla D, Almstead LL, Steitz JA, DiMaio D. miR-29 and miR-30 regulate B-Myb expression during cellular senescence. *Proc Natl Acad Sci U S A.* 2011;108(2):522-527.
49. Duisters RF, Tijsen AJ, Schroen B, et al. miR-133 and miR-30 regulate connective tissue growth factor: implications for a role of microRNAs in myocardial matrix remodeling. *Circ Res.* 2009; 104(2):170-178.
50. Lin J, Lwin T, Zhao JJ, et al. Follicular dendritic cell-induced microRNA-mediated up-regulation of PRDM1 and downregulation of BCL-6 in non-Hodgkin's B-cell lymphomas. *Leukemia.* 2011; 25(1):145-152.

Downloaded from http://ashpublications.org/blood/article-pdf/120/25/5063/1359076/zh805112005063.pdf by guest on 19 May 2024